

Kinematics and Metallicities of Globular Clusters in M104

T.J. Bridges^{1,6}, K.M. Ashman², S.E. Zepf^{3*} †, D. Carter^{1*},
D.A. Hanes^{4*}, R.M. Sharples^{5*}, and J.J. Kavelaars^{4*}

¹*Royal Greenwich Observatory, Madingley Road, Cambridge, England, CB3 0EZ*

²*Dept. of Physics & Astronomy, University of Kansas, Lawrence, KS, USA*

³*Astronomy Dept, Univ. of California, Berkeley, CA, USA*

⁴*Physics Dept, Queen's University, Kingston, Ontario, Canada*

⁵*Dept. of Physics, University of Durham, Durham*

⁶*E-mail: tjb@ast.cam.ac.uk*

Accepted 20 August 1996. Received 23 May 1996.

ABSTRACT

We have obtained spectra for globular cluster candidates in M104 with LDSS-2 on the William Herschel Telescope, confirming 34 objects as M104 globular clusters. We find a cluster velocity dispersion of ~ 260 km/sec, and the Projected Mass Estimator gives a mass of $5.0 (3.5, 6.7) \times 10^{11} M_{\odot}$ for M104 within a projected radius of $\sim 330''$ (14 kpc for $D=8.55$ Mpc). Our best estimate for the mass-to-light ratio is $M/L_{V_T} = 16^{+5.5}_{-5.0}$ within the same radius. Considering all of the possible sources of uncertainty, we find a lower limit of $M/L_V = 5.3$, which is larger than the M/L_V found from rotation curve analyses inside $180''$. We thus conclude that the mass-to-light ratio increases with radius, or in other words that M104 possesses a dark matter halo. There is a marginal detection of rotation in the M104 cluster system at the 92.5% confidence level; larger samples will be needed to investigate this possibility. Interestingly, the M104 globular cluster and planetary nebulae (PNe) kinematics are roughly consistent inside $\sim 100''$. Finally, we find a mean cluster metallicity of $[Fe/H] = -0.70 \pm 0.3$, which is more typical of clusters in *gE/cD* galaxies than it is of clusters in other spirals.

Key words: globular clusters: kinematics, metallicities; galaxies: masses, M/L ratios

1 INTRODUCTION

Globular cluster spectra provide an excellent means to study the kinematics and metallicities of old stellar populations, and to probe the mass distributions of their parent galaxies (see Brodie 1993 and Zepf 1995 for recent reviews). Globular clusters and planetary nebulae (PNe) bridge the gap between the inner regions of ellipticals and early-type spirals, where masses and M/L ratios can be determined from rotation curve work or integrated light techniques, and the outermost regions which can be studied via X-ray emission from hot gas.

In our Galaxy, it is well-known that two globular cluster populations exist—a rapidly rotating, metal-rich disk, and a slowly rotating and metal-poor halo (Zinn 1985; Armandroff

& Zinn 1988; Armandroff 1989). The same situation appears to hold in M31, though this is more controversial (Huchra 1993; Ashman & Bird 1993). In M33, there is no significant rotation in the old, metal-poor clusters (Schommer et al. 1991). To date, M81 is the only late-type galaxy outside the Local Group with measured cluster velocities. Perelmuter, Brodie & Huchra (1995) obtained velocities for 25 clusters out to 20 kpc from the galaxy center, and found a mass of $\sim 3 \times 10^{11} M_{\odot}$ for M81 within the same radius using the Projected Mass Estimator (PME). Their data “cannot be used to demonstrate rotation” in the cluster system, though the cluster velocities are consistent with the HI rotation curve.

There exist a handful of ellipticals with measured cluster velocities: NGC 5128 (87: Harris, Harris & Hesser 1988), NGC 1399 (47: Grillmair et al. 1994), M87 (44), and M49 (26) (Mould et al. 1987, 1990). For M87 and M49, the cluster system has a rotation of ~ 200 km/sec (for *all* clusters combined—no separation has been done by colour/metallicity). There is *no* rotation seen in the metal-poor clusters in NGC 5128 and NGC 1399, while there is significant rotation seen in their PNe at a level of 100–300

* Visiting Astronomer, William Herschel Telescope. The WHT is operated on the island of La Palma by the Royal Greenwich Observatory at the Spanish Observatorio del Roque de los Muchachos of the Instituto de Astrofísica de Canarias.

† Hubble Fellow

km/sec (Hui et al. 1995, Arnaboldi et al. 1994). In NGC 5128, the *metal-rich* cluster population identified by Zepf & Ashman (1993) is observed to rotate like the PNe. Such kinematical differences between clusters and PNe are extremely provocative, and we will return to this point later.

M104 (NGC 4594; the Sombrero) has been well-studied spectroscopically in its inner regions (see Table 1 for basic properties of M104). Faber et al (1977) and Schweizer (1978) derived major axis rotation curves from ionized gas, stellar absorption lines and 21cm emission. Schweizer found a rotation velocity of $\sim 300\text{--}350$ km/sec between 5–15 kpc, and a total mass of $3.3 \times 10^{11} M_{\odot}$ and a M/L_B of 4.9 ± 1.2 within 15 kpc. These values are all in reasonable agreement with those found by Faber et al. Kormendy & Illingworth (1982) obtained the velocity and velocity dispersion profiles along the M104 major axis from optical absorption lines, finding that V flattens out at ~ 250 km/sec between 40–120'' from the galaxy center, while σ flattens out to ~ 100 km/sec at the same distance. These values are in good agreement with those found by Kormendy (1988), Jarvis & Dubath (1988), and Hes & Peletier (1993), although these authors were more interested in the behavior very near the galaxy center.

Most authors have not found any rotation around the minor axis, with the exception of Hes & Peletier who did find some minor axis rotation. Kormendy & Westpfahl (1989) showed that $2 \leq M/L_V \leq 4$ between $0.5 \leq r \leq 180''$. Hes & Peletier found absorption-line strength gradients along the major axis, and concluded on the basis of these gradients and the central kinematics that the M104 bulge is similar in many respects to a giant elliptical. Jarvis & Freeman (1985) constructed models which showed that the surface brightness profiles and kinematics are consistent with the M104 bulge being an isotropic oblate spheroid, flattened mostly by rotation, *unlike* the case for ellipticals of the same luminosity. Jarvis & Freeman found a $M/L_V = 3.6$ within $\sim 80''$, and a disk/bulge ratio of ~ 0.25 for M104. Finally, Burkhead (1986) has carried out a major photometric study and decomposition of M104.

Previous photometric studies of the M104 globular clusters include Wakamatsu (1977), Harris et al. (1984), and Bridges & Hanes (1992). The last two studies found a cluster specific frequency S_N of 2–3, while Bridges et al. estimated the clusters to have $[\text{Fe}/\text{H}] \simeq -0.8$ from B–V colours, a metallicity higher than that found for the clusters in the Milky Way and other nearby spirals.

Globular cluster candidates for spectroscopic analysis were selected in two ways. First, the COSMOS team carried out astrometry and crude photometry on ‘V’ (AAT 1853, IIaD + GG485) and ‘B’ (AAT 1859, IIIaJ + GG385) AAT plates, giving internal positions for thousands of objects. The HST Guide Star Catalogue was then used to identify a set of several dozen stars which were picked by COSMOS, allowing a transformation to absolute coordinates to better than $0.2''$ rms. COSMOS had trouble detecting and measuring objects close to the galaxy bulge, but we also had B,V CCD photometry covering three small patches of the M104 bulge (Bridges & Hanes 1992). These photometrically calibrated data then allowed us to crudely calibrate the COSMOS data by magnitude and colour, and to establish the astrometric scales in the CCD data so that we could add a few near-central objects to our target lists. Final object selection was made on the basis of stellar appearance, and

Table 1. Basic and Derived Information about M104.

Quantity	Value	Reference
RA (1950)	12 37 22.80	1
Dec (1950)	−11 21 00.0	1
V_{hel}	1091 km/sec	1
Hubble Type	Sa ⁺ /Sb [−]	2
M_B	−20.4	3
Adopted Distance	8.55 Mpc	4
Specific Frequency	2 ± 1	5
Cluster $[\text{Fe}/\text{H}]$	-0.7 ± 0.3	6
M/L_{BT}	$22^{+7.5}_{-6.5}$	6

References

- (1) NASA/IPAC Extragalactic Database (NED)
- (2) Sandage & Tammann (1981)
- (3) Burkhead (1986), taking $D=8.55$ Mpc
- (4) Ciardullo, Jacoby, & Tonry (1993)
- (5) Bridges & Hanes (1992)
- (6) This work

by cuts in magnitude and colour. In all, 103 candidates in 3 fields were obtained, extending in radius between 0.8 to 6.2 arcmin from the galaxy center. The LEXT package was used to produce input x, y files which were then used to produce the punched masks. A slit width of $1.5''$ was used, and the slit length varied between 10–60 arcsec.

2 DATA

2.1 Observations and Data Reduction

Spectra for 76 cluster candidates in two of these fields were obtained with the Low Dispersion Survey Spectrograph (LDSS-2) in April 1994; see Table 2 for further details of the observing. Dome and twilight flats were taken at the beginning and end of each night, and CuAr arcs were taken throughout each night. Finally, long-slit spectra of M13, M92, NGC 6356, and radial velocity standard stars were taken for velocity and metallicity calibration. Except where indicated, the LEXT package was used for all data reduction. First, the MAKEFF task was used to produce a dome-flat of mean unity, which was then divided into all of the program frames. After checking to ensure that there were no spatial or spectral shifts between the program frames, the LCCDSTACK program (kindly supplied by Karl Glazebrook) was used to combine the program frames for each mask in an optimal way; all cosmic rays were removed during the stacking. Wavelength calibration was then done using the ARC task on the CuAr exposures; a 3rd order polynomial was found to give a satisfactory fit with residuals typically $\leq 0.1 \text{ \AA}$. Finally, the spectra were optimally extracted and sky subtracted, generally with linear fits for the background sky. 71 spectra were extracted in total, though many of the spectra are of low S/N. Figure 1 shows representative spectra ranging from low to high S/N for three confirmed globular clusters.

Table 2. Observing Log

Dates	April 11-14 1994
Telescope/Instrument	4.2m WHT/LDSS-2
Dispersion (Resolution)	2.4 Å/pixel (6 Å FWHM)
Detector	1024 ² TEK CCD
Wavelength Coverage	3800–5000 Å
Seeing	1–2''
Exposure time (Mask #1/#2)	4.5/2.5 hr
Mean Airmass (Mask #1/#2)	1.4/1.5
Number Objects (Mask #1/#2)	44/32

2.2 Radial Velocities and Confirmed Globular Clusters

The extracted spectra were first scrunched onto a log wavelength scale and then cross-correlated with template spectra of M13, M92, NGC 6356 and HD172, using the IRAF FXCOR task. By experimentation, we found that cross-correlations with peak heights less than 0.1 were not reliable, and hence were not used. We further demanded that bona-fide globular clusters have two or more reliable cross-correlations. Table 3 shows our final velocities for the 71 extracted spectra in the two fields. The velocity shown in Table 3 is the mean (weighted by the cross-correlation peak height) for the four templates; ‘?’ means that no spectrum was extracted and ‘**’ signifies that no reliable cross-correlation could be obtained.

A word on velocity *uncertainties* is in order. The errors given in Table 3 are merely the rms amongst the four templates. We do not have a good idea of the *external* uncertainties. There is one object in common between the two masks (# 1–1 = 2–1), with a velocity difference of 95 km/sec—however, it is a foreground object (we were not able to observe our third field in M104, which had several objects in common with the other two, because of the higher priority placed on NGC 4472, our principal target). For lack of information, we assume velocity errors of 50–100 km/sec, values found from other data of comparable S/N (e.g. M81: Perelmuter, Brodie, & Huchra 1995; M87 & M49: Mould et al. 1990). In any event, even velocity errors of 100 km/sec have little effect on our mass and M/L determinations, given that the observed velocity dispersion of our confirmed cluster sample is ~ 250 km/sec (Section 3.1 below).

In order to isolate a sample of true globular clusters, we subjected the velocity distribution of the (46) objects in Table 3 with reliable velocities (see Figure 2) to the KMM mixture modelling analysis (McLachlan & Basford 1988; Ashman, Bird, & Zepf 1994). This analysis found a best fit of 3 groups—one high velocity point (#1–37), a foreground group of 11 objects, and 34 objects with velocities $500 \leq V \leq 1600$ km/sec. Inspection of Figure 2 suggests that this is a sensible split. The last column of Table 3 shows which objects are confirmed globular clusters; there are 34 such objects in total.

3 RESULTS

Table 3. Velocities of Globular Cluster Candidates in M104. Successive columns give Id #, Ra, Dec, Velocity, and Velocity Error, for 44 cluster candidates in Field #1. A ‘?’ means that no spectrum could be extracted, and a ‘**’ means that no reliable cross-correlation could be obtained. There are 34 confirmed globular clusters (see last column).

Id	Ra (1950)	Dec (1950)	V_{hel} (km/s)	Error (km/s)	Cluster?
1–1	12 37 40.460	-11 21 33.55	212	18	N
1–2	12 37 34.548	-11 20 18.29	776	11	Y
1–3	12 37 35.516	-11 21 47.40	1369	129	Y
1–4	12 37 33.716	-11 18 53.53	1152	40	Y
1–5	12 37 34.864	-11 19 27.65	755	61	Y
1–6	12 37 26.784	-11 18 10.02	109	20	N
1–7	12 37 28.576	-11 19 8.93	**	**	N
1–8	12 37 27.544	-11 16 14.52	**	**	N
1–9	12 37 28.896	-11 17 36.80	194	29	N
1–10	12 37 36.140	-11 24 20.96	-51	21	N
1–11	12 37 28.848	-11 19 54.47	1457	12	Y
1–12	12 37 37.988	-11 22 11.38	1370	32	Y
1–13	12 37 36.624	-11 18 30.11	219	78	N
1–14	12 37 33.112	-11 17 0.81	**	**	N
1–15	12 37 35.600	-11 25 29.50	1035	24	Y
1–16	12 37 39.288	-11 21 7.67	1256	18	Y
1–17	12 37 35.336	-11 22 26.42	**	**	N
1–18	12 37 12.224	-11 24 59.35	**	**	N
1–19	12 37 20.336	-11 21 58.89	573	21	Y
1–20	12 37 5.104	-11 19 40.84	1186	51	Y
1–21	12 37 35.580	-11 16 37.59	**	**	N
1–22	12 37 31.244	-11 22 56.33	131	43	N
1–23	12 37 41.120	-11 25 3.76	**	**	N
1–24	12 37 24.920	-11 23 12.60	??	??	N
1–25	12 37 7.988	-11 21 2.23	1231	26	Y
1–26	12 37 28.316	-11 23 51.23	1199	14	Y
1–27	12 37 3.460	-11 24 23.50	-233	26	N
1–28	12 37 18.652	-11 24 8.86	932	25	Y
1–29	12 37 37.460	-11 22 45.05	853	31	Y
1–30	12 37 17.232	-11 23 25.00	**	**	N
1–31	12 37 6.112	-11 16 49.60	**	**	N
1–32	12 37 14.744	-11 22 27.14	1025	203	Y
1–33	12 37 25.420	-11 20 5.94	448	141	N
1–34	12 37 11.292	-11 18 24.53	-31	6	N
1–35	12 37 16.768	-11 22 43.71	1300	40	Y
1–36	12 37 35.436	-11 26 11.98	**	**	N
1–37	12 37 14.296	-11 16 37.64	2456	24	N
1–38	12 37 18.800	-11 24 42.64	**	**	N
1–39	12 37 6.072	-11 18 55.96	832	61	Y
1–40	12 37 26.668	-11 25 16.04	**	**	N
1–41	12 37 7.676	-11 20 24.56	**	**	N
1–42	12 37 3.752	-11 23 11.61	**	**	N
1–43	12 37 16.964	-11 22 14.78	**	**	N
1–44	12 37 41.244	-11 20 52.17	**	**	N

3.1 Mass and M/L Ratio

We have used the ROSTAT code (Beers, Flynn, & Gebhardt 1990; Bird & Beers 1993), to obtain robust values for the mean cluster velocity and velocity dispersion. We find that the robust mean velocity (location) is 1074 (–79,+78) km/sec, where we quote boot-strapped 90% confidence intervals. Similarly, the biweight velocity dispersion (scale) is 255 (210, 295) km/sec, where this value has been corrected for a possible rotation of ~ 70 km/sec (Section 3.2.1), and velocity errors of 100 km/sec per point are assumed; we again

Table 3 – *continued* Id #, Ra, Dec, Velocity, and Velocity Errors are given for 32 cluster candidates in Field #2.

Id	Ra (1950)	Dec (1950)	V_{hel} (km/s)	Error (km/s)	Cluster?
2-1	12 37 40.460	-11 21 33.55	306	45	N
2-2	12 37 30.192	-11 20 20.00	808	39	Y
2-3	12 37 36.332	-11 21 45.12	1524	14	Y
2-4	12 37 16.272	-11 19 13.20	968	78	Y
2-5	12 37 31.388	-11 19 24.32	1220	89	Y
2-6	12 37 24.600	-11 18 52.32	1283	45	Y
2-7	12 37 17.976	-11 19 37.71	976	24	Y
2-8	12 37 23.200	-11 22 0.79	979	14	Y
2-9	12 37 39.308	-11 25 25.85	-83	25	N
2-10	12 37 23.312	-11 20 4.55	**	**	N
2-11	12 37 32.396	-11 17 30.21	1411	56	Y
2-12	12 37 13.260	-11 18 7.37	857	42	Y
2-13	12 37 23.720	-11 18 27.38	616	34	Y
2-14	12 37 25.464	-11 22 36.75	1045	7	Y
2-15	12 37 26.900	-11 22 18.79	828	71	Y
2-16	12 37 16.784	-11 19 50.53	875	22	Y
2-17	12 37 35.248	-11 23 16.06	1275	100	Y
2-18	12 37 7.460	-11 23 3.04	**	**	N
2-19	12 37 34.280	-11 16 18.73	??	??	N
2-20	12 37 37.480	-11 22 51.50	**	**	N
2-21	12 37 34.952	-11 24 25.56	**	**	N
2-22	12 37 5.504	-11 23 17.64	??	??	N
2-23	12 37 6.072	-11 24 50.98	??	??	N
2-24	12 37 30.260	-11 23 46.25	1505	119	Y
2-25	12 37 7.380	-11 21 3.77	**	**	N
2-26	12 37 40.516	-11 16 50.78	??	??	N
2-27	12 37 13.332	-11 16 53.25	**	**	N
2-28	12 37 43.736	-11 23 31.64	**	**	N
2-29	12 37 21.284	-11 16 34.38	**	**	N
2-30	12 37 5.916	-11 24 31.71	1104	104	Y
2-31	12 37 15.416	-11 21 48.77	939	21	Y
2-32	12 37 12.236	-11 24 9.03	**	**	N

quote 90% boot-strapped confidence intervals. The correction for possible rotation has been done assuming a step function (cf. Mould et al. 1990, and see Section 3.2.1 and Figure 3); this correction changes σ by only ~ 10 km/sec. The mean velocity is reassuringly close to the recession velocity of M104 itself, which is 1091 ± 5 km/sec (RC3). The M104 cluster velocity dispersion is much larger than that of old clusters in other spiral galaxies (e.g. Milky Way: $\sigma \simeq 100$ km/sec–Armandroff 1989, Da Costa & Armandroff 1995; M31: $\sigma \simeq 150$ km/sec–Huchra 1993; M33: $\sigma \simeq 70$ km/sec–Schommer et al. 1991); M81: $\sigma \simeq 150$ km/sec–Perelmuter, Brodie & Huchra 1995), but smaller than that of gE galaxies (e.g. M87: $\sigma \simeq 385$ km/sec; M49: $\sigma \simeq 330$ km/sec–Mould et al. 1990; NGC 1399: $\sigma \simeq 390$ km/sec–Grillmair et al. 1994). While a direct comparison of these numbers isn’t very meaningful, since they are measured to different radii (or, more physically, scale-lengths) in each galaxy, they do indicate the presence of dark matter halos in these galaxies. In an attempt to see if the cluster velocity dispersion varies with galactocentric radius, we divided the data into 4 radial bins, with roughly equal numbers of clusters in each bin. Unfortunately, the small number of data points and resulting large confidence intervals mean that we cannot place useful constraints on any such variation.

We have used the Projected Mass Estimator (PME) to determine the mass of M104:

$$M_p = \frac{f_p}{NG} \sum_{i=1}^N r_i v_i^2$$

where r_i is the projected galactocentric radius of the i th cluster, and v_i is the velocity corrected for the mean cluster velocity (1074 km/sec). The f_p factor depends on the assumed cluster velocity distribution. We have adopted a value of $f_p = 16/\pi$ which assumes isotropic orbits and a central point mass (Bahcall & Tremaine 1981; Heisler, Tremaine, & Bahcall 1985); for radial and tangential orbits $f_p = 32/\pi$ and $32/3\pi$ respectively. Finally, we have assumed a distance $D = 8.55$ Mpc based on the SBF distance of Ciardullo, Jacoby, & Tonry (1993; Ford et al. 1996 give a slightly higher distance of 8.9 ± 0.6 Mpc, based on the PNLFF) for M104–the mass will scale with D . The robust implementation of the PME gives $M_p = 5.2$ ($3.9, 6.7$) $\times 10^{11} M_\odot$, where we quote 90% boot-strapped confidence intervals, and we have taken the galaxy centroid as the dynamical center. Correcting for velocity errors, possible rotation, and using the clusters themselves to define the dynamical center reduce M_p by $< 10\%$. Thus, we quote $M_p = 5.0$ ($3.5, 6.7$) $\times 10^{11} M_\odot$. The main uncertainties in M_p are the assumptions about the cluster orbital distribution, the M104 distance, and whether or not we use a central point mass or extended mass distribution for M104, all of which are uncertain by roughly a factor of two. We take M_p to be the mass within the projected radius of the furthestmost cluster in our sample, which lies at 5.5 arcmin (14 kpc for $D=8.55$ Mpc).

From Burkhead (1986), the total integrated magnitude of M104 is $B_{tot} = 9.24$ within 5.5 arcmin, where we have corrected for $A_B = 0.12$ mag (Burstein & Heiles 1984). Thus, $L_B (< 5.5') = 2.3 \times 10^{10} L_\odot$ for $D=8.55$ Mpc, and $M/L_{BT} = 22^{+7.5}_{-6.5}$, where the uncertainties reflect only the *formal* confidence intervals for M_p above. Taking $B-V = 1$ (Burkhead 1986), the corresponding $M/L_V = 16^{+5.5}_{-5.0}$. These M/L ratios scale as $\frac{8.55 \text{ Mpc}}{D}$. Given the uncertainties mentioned above, our quoted M/L ratios are probably only believable to within a factor of two.

Do our data imply the existence of dark matter in the M104 halo? Kormendy & Westpfahl (1989) showed that spectroscopic data available at that time yielded $2 \leq M/L_V \leq 4$ between $0.5 - 180''$, assuming a distance of 18 Mpc, and they concluded that there “*is no evidence for halo dark matter between $11 \leq r \leq 215''$* .” From our cluster data, we can obtain a lower bound on the M/L ratio by assuming tangential orbits, a central point mass, and a distance of 18 Mpc: we find that $M/L_V \geq 5.3$ within 5.5 arcmin. Thus, we find that the M/L ratio must increase with radius (by a factor of ~ 4 between $180-330''$ for our best estimate of $M/L_V = 16$), and we conclude that *there is indeed dark matter in the M104 halo*.

Our M/L agrees well with those found from globular clusters in other spirals (e.g. M31: $M/L_B = 16$ –Huchra 1993; M81: $M/L_B = 19$ –Perelmuter, Brodie & Huchra 1995, both within 20 kpc). For some gE/cD galaxies, M/L is larger (cf. M87: $M/L_V = 31$ inside ~ 40 kpc; NGC 1399: $M/L_B \simeq 70-80$ between 20–40 kpc. For other ellipticals, however, the M/L is lower (e.g. M49: $M/L_B \leq 10$ inside 20 kpc; NGC 5128: $M/L_B \simeq 10$).

3.2 Kinematics and Comparison with PNe

3.2.1 Rotation in the Cluster System?

In Figure 3, we show the cluster velocities as a function of distance along the major axis of M104; as discussed in Section 2.2, the error bars are only internal, and the true uncertainties are likely to be 50–100 km/sec. While there is considerable scatter at all radii, there is a *hint* of rotation in the cluster system, with clusters west of the galaxy center having lower velocities on average than those on the eastern side. In Figure 3, the solid line is a linear least squares fit, with a slope of 0.43 km/sec/arcsec. Over the 8 arcmin along the major axis covered by the studied clusters, this amounts to ~ 210 km/sec or a V_{rot} of ~ 105 km/sec. Another way to estimate the possible rotation is to compare the mean cluster velocity east and west of the minor axis. We have done this in a robust way with ROSTAT, since this should be more reliable than a classical Gaussian estimator with the small number of datapoints. We find that the mean velocities for the two datasets are: $V_{east} = 1137$ (–116, +124); $V_{west} = 991$ (–66, +107) km/sec, where the values in brackets are the 90% bootstrapped uncertainties. Therefore, $2V_{rot} = 146_{-133}^{+164}$ km/sec, or $V_{rot} = 73_{-66}^{+82}$ km/sec.

We have also carried out a Mann-Whitney U test on our data. The hypothesis that the velocities of clusters with RA less than that of M104 are drawn from the same population as the velocities of clusters with RA greater than M104 can be rejected at the 92.5% confidence level. In addition, the hypothesis that the velocities of clusters with Dec less than that of M104 are drawn from the same population as the velocities of clusters with Dec greater than M104 cannot be rejected. In other words, there is a correlation between velocity and major axis position (since the M104 major axis lies almost exactly East-West), and no correlation between velocity and minor axis position. We interpret this as a marginal detection of rotation in the cluster system, at the 92.5% confidence level. However, it is clear from Figure 3 that we have large error bars, and there may be considerable real scatter; many more velocities will be needed to resolve this issue.

Rotation at a similar amplitude is observed in the outer, metal-rich M31 clusters ($V_{rot} \sim 70$ km/sec: Huchra 1993). Rotation at lower levels of 40–50 km/sec are found for the metal-rich clusters in M33 (Schommer et al. 1991) and NGC 5128 (Hui et al. 1995), and for the metal-poor Galactic halo and M31 clusters (Da Costa & Armandroff 1995; Huchra 1993), while no significant rotation is detected in the metal-poor M33 clusters (Schommer et al. 1991). It would be extremely interesting to obtain a large sample of high S/N spectra of M104 clusters, so that a similar comparison could be made between the kinematics of metal-poor and metal-rich clusters in that galaxy.

3.2.2 Comparison with M104 PNe

Ken Freeman has very kindly shared preliminary results for 100 PNe velocities in M104 (of ~ 250 total). For those objects within $74''$ of the galactic plane, the PNe show a rotation of 50–100 km/sec out to $\sim 250''$ along the major axis. The PNe velocity dispersion is ~ 220 km/sec at $50''$ radius, dropping off to ~ 180 km/sec between 120 – $150''$ radius. Thus, the PNe and cluster kinematics are roughly con-

sistent in M104, out to $\sim 100''$. The PNe velocity dispersion is slightly lower than that of the globular clusters beyond $\sim 120''$, but this difference is not significant given the uncertainties in the cluster velocity dispersion.

Interestingly, in the two other galaxies for which we can make a direct comparison of cluster and PNe kinematics, NGC 1399 and NGC 5128, there is PNe rotation (~ 300 km/sec and 100 km/sec respectively), yet *no* rotation is seen in the metal-poor clusters. The metal-rich clusters in NGC 5128 have $V \sim 40$ km/sec inside 6 kpc. Arnaboldi et al. (1994) attribute the difference in kinematics in NGC 1399 to a tidal interaction between it and the nearby NGC 1404. N-body work by Barnes (1996) shows that stellar populations preserve some kinematic memory after major merger events, and Barnes speculates that “... if NGC 5128 is the result of a major merger, the planetary nebulae and globular clusters may trace different populations from the original galaxies, with the former exhibiting a kinematic memory of the disks from whence they came.”

3.3 The Mean Cluster Metallicity

Although our cluster spectra are individually too noisy to obtain useful metallicity estimates, the combination of all 34 spectra into one higher S/N spectrum does give a good determination of the mean cluster metallicity. Bridges & Hanes (1992) showed that there is no dependence of mean B–V colour on B magnitude or galactocentric radius; thus, the mean metallicity of our 34 clusters should be representative of the M104 cluster system as a whole. Our individual spectra were shifted using the cross-correlation results, and then added to give the final spectrum shown in Figure 4. Ca H&K, H δ , G-band and H γ are all clearly seen.

For quantitative analysis, we have used the G-band equivalent width (EW) to determine [Fe/H]; the G-band is one of Brodie & Huchra’s (1990; BH hereafter) 6 primary metallicity indicators. Following their prescription, we fit the continuum on two segments between 4284–4300 Å and 4336–4351 Å, and calculate the feature EW between 4300–4333 Å. Using the FIGARO ABLINE routine, we find a central wavelength of 4317 Å and an EW of 4.40 Å. We then convert this EW into the BH feature index I via $I = -2.5 \log(1 - EW/\delta\lambda)$, yielding $I = 0.155$. Finally, we use the BH calibration between G-band strength and [Fe/H], as determined from calibrating clusters in the Milky Way and M31, to estimate [Fe/H]. We find $[Fe/H] = -0.70 \pm 0.30$, where the uncertainty is taken from the scatter in the BH calibration (their Table 7).

There is another BH primary index that falls within our bandpass: Δ , which measures the line-blanketing discontinuity at 4000 Å. (Note that the CNB feature, between 3810–3910 Å is also within our bandpass, but we lack a continuum passband shortwards of this feature). Unfortunately, our lack of flux calibration (due to the difficulties of flux-calibrating multi-slit spectra) makes broad metallicity indices such as Δ unreliable. BH list H+K (the Calcium H & K lines) as one of their “poorer” calibrators, but it is useful as a consistency check on our G-band metallicity. We measure an EW of 16.0 Å for H+K (feature between 3935–3995 Å, and continuum fitted between 3920–3935 and 4000–4010 Å), which translates into $[Fe/H] = -0.55 \pm 0.4$, where again we have taken the uncertainty from the scatter

Table 4. Mean [Fe/H] metallicity of globular cluster systems as a function of parent galaxy luminosity. This Table has been adapted from Figure 7 of Secker et al. (1995). Data for M104 taken from this paper, for M81 from Perelmuter, Brodie, & Huchra (1995), and for other spirals from Harris (1991). Globular cluster data for NGC 1399 from Ostrov et al. (1993), for M87 from Lee & Geisler (1993), for NGC 3923 from Zepf et al. (1995), for NGC 6166 from Bridges et al. (1996), and for remaining E galaxies from Harris (1991).

Galaxy	M_{V_T}	Mean Cluster [Fe/H]	uncertainty
E/gE			
NGC 1399	-21.1	-0.90	0.20
NGC 3311	-22.8	-0.34	0.30
NGC 4486	-22.4	-0.86	0.20
NGC 3923	-22.05	-0.55	0.20
NGC 4472	-22.6	-0.80	0.30
NGC 4649	-22.2	-1.10	0.20
NGC 5128	-22.0	-0.84	0.10
NGC 6166	-23.6	-1.00	0.30
Spirals			
M104	-22.1	-0.70	0.30
M33	-19.2	-1.40	0.20
MW	-21.3	-1.35	0.05
M31	-21.7	-1.21	0.05
M81	-21.0	-1.50	0.20
NGC 3031	-21.2	-1.46	0.31

in the BH calibration. Though the H+K determination has larger scatter, it is consistent with the G-band value.

The mean cluster [Fe/H] agrees well with that estimated previously by Bridges & Hanes (1992), who found [Fe/H] = -0.8 ± 0.25 from B–V colours of ~ 130 cluster candidates with $0.3 \leq B-V \leq 1.3$. It is encouraging to see the agreement between spectroscopic and photometric metallicities. As we show in Table 4, the M104 globular clusters are seen to be considerably more metal-rich than those of other spirals; Table 4 also shows that M104 is comparable to E/gE galaxies both in luminosity and mean cluster [Fe/H].

Much of the recent discussion about a possible relationship between galaxy luminosity and mean cluster metallicity has focussed on elliptical galaxies. It is instructive to see if there is any such relationship for spirals alone. Figure 5 shows the data for the 6 spirals in Table 4. Over the small magnitude range $-21 \leq M_V \leq -22$, there does seem to be a trend, though this is largely driven by our new data for M104. By contrast, there seems to be considerably more scatter about any possible relationship for E/gE galaxies (cf. Secker et al 1995). This difference between spirals and ellipticals would be expected if most ellipticals are created by mergers. During a merger a new generation of clusters of higher metallicity may be created (AZ), and the galaxy luminosity will change, creating more scatter in both M_V and cluster [Fe/H]. Spirals, however, have presumably not experienced major merger events, and will adhere more closely to any “primordial” M_V –[Fe/H] relation. However, M104 is not a typical spiral: it is very bright and its disk is a minor com-

ponent; it is thus not clear if it should be included in Figure 4. M33 is also unusual in the other extreme, since it has very little stellar bulge yet has managed to produce a significant cluster population (e.g. Bothun 1992). More metallicities for globular clusters in spiral galaxies are urgently needed.

4 CONCLUSIONS

We have obtained spectra for 76 globular cluster candidates in M104. 34 of these objects have been confirmed as M104 globular clusters from their spectra and radial velocities; this sample extends out to ~ 5.5 arcmin in projected radius (14 kpc for our adopted distance of $D=8.55$ Mpc). Our main conclusions are as follows:

(1): The cluster velocity dispersion is 255 (210, 295) km/sec, after correction for possible rotation of the cluster system. This result confirms that M104 is a very massive spiral, as would be inferred from its luminosity.

(2): The Projected Mass Estimator yields a mass of $5.0 (3.5, 6.7) \times 10^{11} M_\odot$ for M104, within a projected radius of 5.5 arcmin (14 kpc). The corresponding mass-to-light ratio is $M/L_{B_T} = 22^{+7.5}_{-6.5}$ ($M/L_{V_T} = 16^{+5.5}_{-5.0}$), assuming isotropic orbits and a central point mass for M104. Although there are considerable uncertainties in this M/L determination, we believe that our quoted value is at the low end of the allowed range. Comparing to the $M/L_V \leq 4$ found from stellar and HI rotation curves within $200''$, our best estimate is that the M/L ratio of M104 increases with radius, as would be expected if the galaxy was surrounded by a dark matter halo.

(3): There is a marginal detection of rotation in the M104 globular cluster system at the 92.5% confidence level. However, many more cluster velocities are required to conclusively establish rotation. The kinematics of the clusters are roughly consistent with preliminary results of Freeman et al. for the M104 PNe.

(4): The mean globular cluster metallicity as determined from the G-band equivalent width of the composite cluster spectrum is [Fe/H] = -0.70 ± 0.3 , using the calibration of Brodie & Huchra (1990). This metallicity is higher than that of clusters in other spiral galaxies, but comparable to that of E/gE galaxies of similar luminosity to M104.

ACKNOWLEDGEMENTS

We would like to acknowledge Harvey MacGillivray for doing the COSMOS scans, and Dave Malin for expediting the delivery of the M104 plates to Edinburgh. We thank Ken Freeman and his collaborators for sharing preliminary results from their M104 PNe data. We are grateful to Nial Tanvir and Karl Glazebrook for all of their help with LEXT. Many thanks go to Tina Bird for her assistance with RO-STAT and all things robust. We appreciate the useful discussions with Joe Haller and Scott Tremaine regarding the use of the Projected Mass Estimator. We also acknowledge the assistance of Peter Bleackley in data reduction. SEZ acknowledges support from NASA through grant number HF-1055.01-93A awarded by the Space Telescope Science Institute, which is operated by the Association of Universities for Research in Astronomy, Inc., for NASA under contract

NASA-26555. DAH and JJK acknowledge NSERC for support through an Operating Grant provided to DAH. This research has made use of the NASA/IPAC Extragalactic Database (NED) which is operated by the Jet Propulsion Laboratory, California Institute of Technology, under contract with the National Aeronautics and Space Administration.

REFERENCES

- Armandroff, T.E., 1989, AJ, 97, 375
 Armandroff, T.E., Zinn, R., 1988, AJ, 96, 92
 Arnaboldi, M., Freeman, K.C., Hui, X., Capaccioli, M., Ford, H., 1994, *Eso Messenger*, 76, 40
 Ashman, K.M., Bird, C.M., Zepf, S.E., 1994, AJ, 108, 2348
 Ashman, K.M., Bird, C.M., 1993, AJ, 106, 2281
 Bahcall, J.N., Tremaine, S., 1981, ApJ, 244, 805
 Barnes, J.E., 1996, in *Formation of the Galactic Halo ... Inside and Out*, ASP Conference Series #92, eds. H. Morrison & A. Sarajedini, (ASP: San Francisco), pg. 415
 Beers, T.C., Flynn, K., Gebhardt, K., 1990, AJ, 100, 32
 Bird, C.M., Beers, T.C., 1993, AJ, 105, 1596
 Bothun, G.D., 1992, AJ, 103, 104
 Bridges, T.J., Hanes, D.A., 1992, AJ, 103, 800
 Bridges, T.J., Carter, D., Harris, W.E., Pritchett, C.J., 1996, MNRAS, in press
 Brodie, J.P., 1993, in *The Globular Cluster-Galaxy Connection*, ASP Conference Series #48, pg. 483
 Brodie, J.P., Huchra, J.P., 1990, ApJ, 362, 503 (BH)
 Burkhead, M.S., 1986, AJ, 91, 777
 Burstein, D., Heiles, C., 1984, ApJS, 54, 33
 Ciardullo, R., Jacoby, G.H., Tonry, J.L., 1993, ApJ, 419, 479
 Da Costa, G.S., Armandroff, T.E. 1995, AJ, 109, 2533
 Faber, S.M., Balick, B., Gallagher, J.S., Knapp, G.R., 1977, ApJ, 214, 383
 Grillmair, C.J., Freeman, K.C., Bicknell, G.V., Carter, D., Couch, W.J., Sommer-Larsen, J., Taylor, K., 1994, ApJ, 422, 9
 Harris, W.E., 1991, ARA&A, 543
 Harris, W.E., Harris, H.C., Harris, G.L.H., 1984, AJ, 89, 216
 Harris, H.C., Harris, G.L.H., Hesser, J.E., 1988, in *The Harlow-Shapley Symposium on Globular Cluster Systems in Galaxies*, pg. 205
 Heisler, J., Tremaine, S., Bahcall, J.N., 1985, ApJ, 298, 8
 Hes, R., Peletier, R.F., 1993, A&A, 268, 539
 Huchra, J.P., 1993, in *The Globular Cluster-Galaxy Connection*, ASP Conference Series #48, pg. 420
 Hui, X., Ford, H.C., Freeman, K.C., Dopita, M.A., 1995, ApJ, 449, 592
 Jarvis, B.J., Freeman, K.C. 1985, ApJ, 295, 324
 Jarvis, B.J., Dubath, P., 1988, A&A, 201, 33
 Kormendy, J., 1988, ApJ, 335, 40
 Kormendy, J., & Illingworth, G., 1982, ApJ, 245, 460
 Kormendy, J., & Westpfahl, D.J., 1989, ApJ, 338, 752
 Lee, M.G., Geisler, D., 1993, AJ, 106, 493
 McLachlan, G.J., Basford, K.E., 1988, in *Mixture Models: Inference and Applications to Clustering*, (Marcel Dekker, New York).
 Mould, J.R., Oke, J.B., Nemec, J.M., 1987, AJ, 93, 53
 Mould, J.R., Oke, J.B., de Zeeuw, P.T., Nemec, J.M., 1990, AJ, 99, 1823
 Ostrov, P., Geisler, D., Forte, J.C., 1993, AJ, 105, 1762
 Perelmuter, J., Brodie, J.P., Huchra, J.P., 1995, AJ, 110, 620
 Sandage, A., Tammann, G.A., 1981, *A Revised Shapley-Ames Catalog of Bright Galaxies*, Carnegie Institution of Washington Publication No. 635, Washington, DC
 Schommer, R.A., Christian, C.A., Caldwell, N., Bothun, G.D., Huchra, J.A., 1991, AJ, 101, 873
 Secker, J., Geisler, D., McLaughlin, D.E., Harris, W.E., 1995, AJ, 109, 1019
 Schweizer, F., 1978, ApJ, 220, 98
 Wakamatsu, K.I., 1977, PASP, 89, 267
 Zepf, S.E. 1995, in *Dark Matter*, eds. S.S. Holt & C.L. Bennett, (AIP: New York), pg. 153
 Zepf, S.E., Ashman, K.M., 1993, MNRAS, 264, 611
 Zepf, S.E., Ashman, K.M., Geisler, D., 1995, ApJ, 443, 570
 Zinn, R., 1985, ApJ, 293, 424

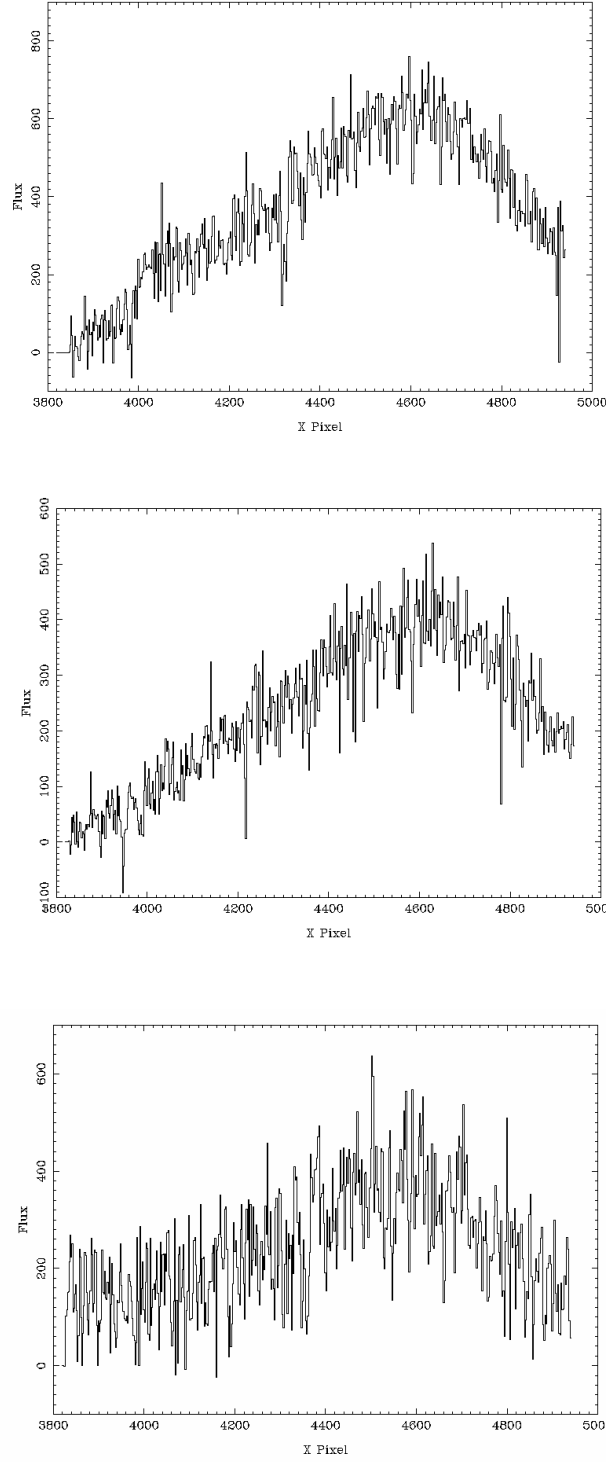


Figure 1. Representative Spectra of M104 Globular Clusters. The top, middle and bottom panels show spectra of high (#1–8), average (#2–9), and low (#1–36) S/N, respectively. Units along the X axis are in \AA , while the Y axis units are in counts.

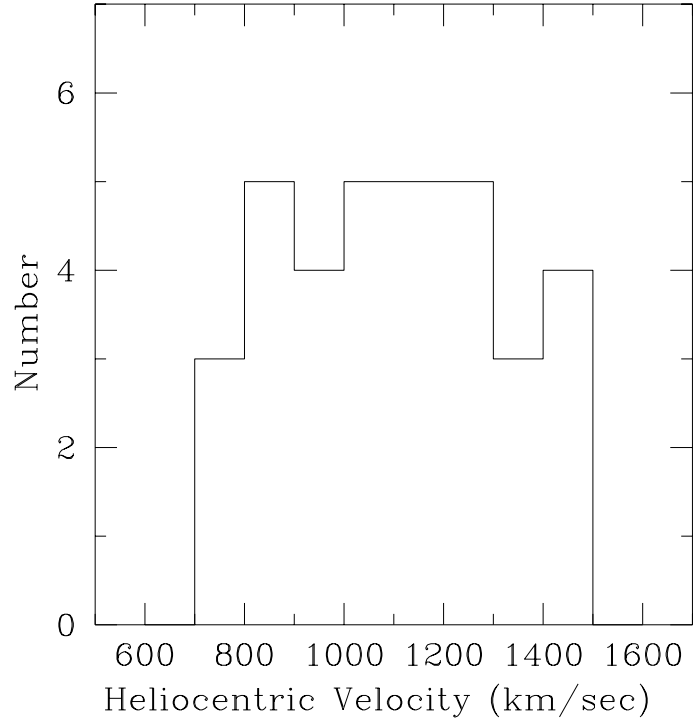


Figure 2. Velocity Histogram of (34) Confirmed M104 Globular Clusters.

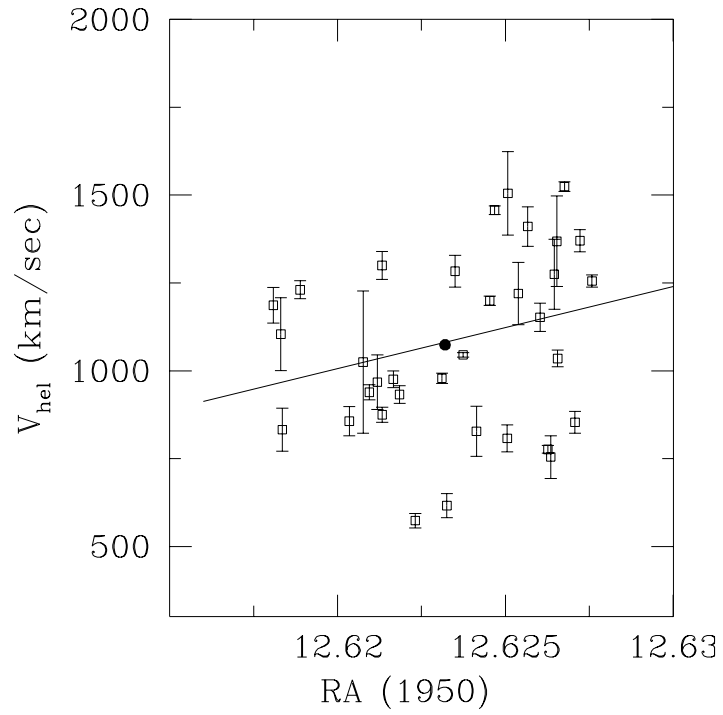


Figure 3. Globular Cluster Velocity vs. Major Axis Radius. The black circle denotes the galaxy center.

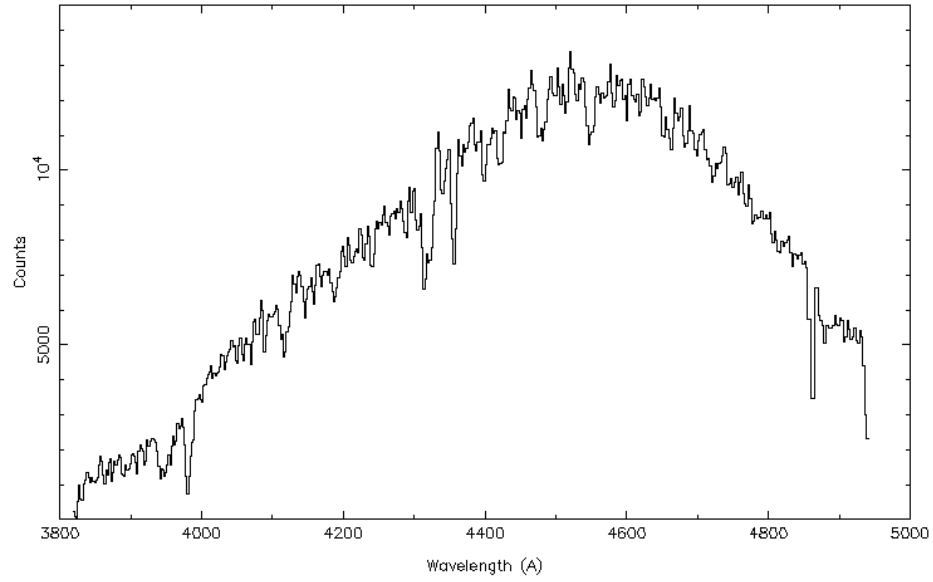


Figure 4. Co-added Spectrum of (34) confirmed M104 globular clusters.

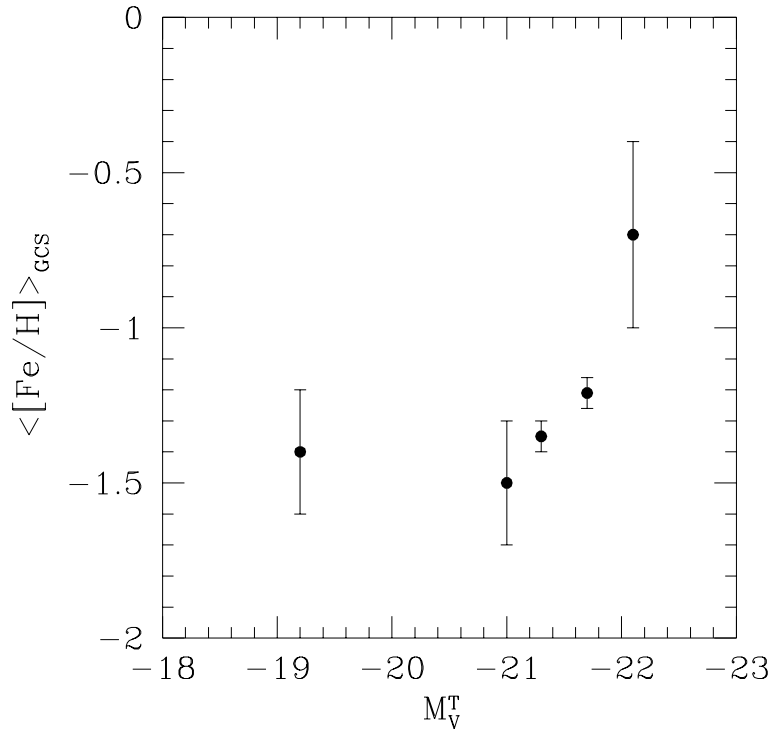


Figure 5. Mean Cluster $[Fe/H]$ vs. Parent Galaxy Luminosity (M_{V_T}) for spiral galaxies.